Biotransformation of the triketone herbicide Mesotrione by a Bacillus strain. Metabolite profiling using liquid chromatography/electrospray ionization quadrupole-time of flight mass spectrometry.

Stéphanie Durand, Bertrand Legeret, Anne-Sophie Martin, Martine Sancelme, A.M. Delort, Pascale Besse-Hoggan, Bruno Combourieu

Biotransformation of the triketone herbicide mesotrione by a *Bacillus* strain. Metabolite profiling using liquid chromatography/electrospray ionization quadrupole time-of-flight mass spectrometry

Stéphanie Durand, Bertrand Légeret, Anne-Sophie Martin, Martine Sancelme, Anne-Marie Delort, Pascale Besse-Hoggan and Bruno Combourieu*

Laboratoire de Synthèse et Etude de Systèmes à Intérêt Biologique, UMR 6504 CNRS, Université Blaise Pascal, 63177 Aubière Cedex, France

Received 11 May 2006; Revised 21 June 2006; Accepted 21 June 2006

The metabolic pathway involved in the biotransformation of the herbicide mesotrione by the bacterial strain *Bacillus* sp. 3B6 was investigated by a reliable liquid chromatography/electrospray ionization quadrupole time-of-flight mass spectrometry (LC/ESI-QTOF-MS) method. The LC/ESI-MS method, both in positive and negative mode, with the assistance of MS^2 fragments and isotopic pattern analyses, allowed us to identify five metabolites. This work constitutes the first complete monitoring of mesotrione degradation kinetics. Among the transformation products found by both techniques, one was formed by intramolecular cyclization between a hydroxylamine and a keto function, which is quite a rare biological reactivity process. For each identified metabolite, a fragmentation pathway is proposed for negative and positive mode. Copyright © 2006 John Wiley & Sons, Ltd.

Mesotrione [2-(4-methylsulfonyl-2-nitrobenzoyl)-1,3-cyclohexanedione] (Fig. 1) is a new selective herbicide for control of broad-leaved weeds in maize, reportedly targeted to replace atrazine which has been banned in several European countries in recent years.[1] Indeed the agrochemical consumption of mesotrione is increasing regularly. To date, however, few data only are available concerning the fate of mesotrione. Therefore, predicting the fate of this herbicide and its metabolites in the environment is of social and environmental concern.

We have very recently published the first isolation and identification of a pure bacterial strain (*Bacillus* sp. 3B6) able to transform mesotrione.[2] Only AMBA [2-amino-4-methylsulfonylbenzoic acid] was identified as a metabolite of this strain although MNBA [4-methylsulfonyl-2-nitrobenzoic acid] was also proposed in the few studies described in the literature (Fig. 1).[3–6] Indeed, MNBA and AMBA were identified by high-performance liquid chromatography/ultraviolet (HPLC-UV) in soil treated by mesotrione, after solid-phase extraction. However, no other compound was observed by this approach, and the ratio of each metabolite could not be determined. Consequently, the detailed metabolic pathway of mesotrione is not yet completely known since no kinetic study has been reported previously. Information on metabolites formed during biotransformation using pure microbial strains can be valuable for comprehensive assessment of the fate of the parent herbicide and its metabolites in the environment.

In the present work, liquid chromatography/electrospray ionization quadrupole time-of-flight mass spectrometry (LC/ESI-QTOF-MS) was performed to identify the intermediate and final products of the biodegradation of mesotrione by *Bacillus* sp. 3B6 in resting cell experiments. QTOF has become one of the most popular analyzers to screen metabolic fingerprints and thus to determine the metabolic pathways (with no preconceptions) even of low molecular weight compounds.[7–10]

The purpose of the present study was to collect new data concerning mesotrione biotransformation and to identify new metabolites. Since no data were available in the literature concerning ESI fragmentation of such a family of compounds, we focused our attention on ion fragmentations for both mesotrione and its metabolites and mass spectral patterns. The structures of unknown compounds were deduced from their MS^2 spectra as well as elemental compositions. Moreover, isotopic patterns confirmed the presence of a sulfur atom in the structure. The chromatographic conditions used had to be suitable for both sensitivity and detection of differently charged unknown compounds at a significant level (down to 100 nM in raw samples). Five metabolites were thus identified, among which four had never been described previously.

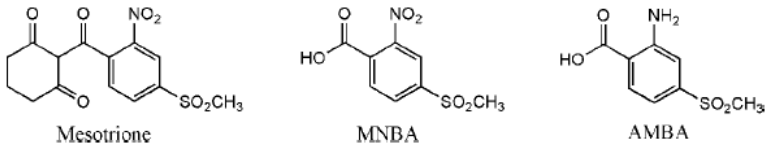

Figure 1. Molecular structures of mesotrione, MNBA and AMBA.

EXPERIMENTAL

Degradation of mesotrione by the isolated strain *Bacillus* sp. 3B6

The bacterial strain *Bacillus* sp. 3B6 used in this study was isolated and characterized as previously described.[2] The resting cells (grown on Trypcase-Soy broth medium for 24 h at 27°C and prepared as previously described[2]) were incubated with 1 or 5 mmol/L mesotrione in 500 mL Erlenmeyer flasks at 27°C with agitation (200 rpm). Samples (1 mL) were taken regularly and centrifuged at 12 000 *g* for 5 min. Supernatants were immediately frozen until analysis by LC-UV-MS. In some cases, samples were analyzed directly without freezing to check and/or avoid abiotic degradation of some of the metabolites.

Each biotransformation experiment was repeated four times and analyzed independently by LC/ESI-MS and LC/ESI-MS/MS. For each experiment, a total of six points, corresponding to different incubation times, was studied. Metabolite profiles were identical for all assays. Control experiments were carried out, i.e. cells without mesotrione and mesotrione alone. No metabolite was observed in these controls.

HPLC conditions

All solvents were LC/MS grade (J.T. Baker Laboratories, Atlantic Labo, Eysines, France). The HPLC-UV and HPLC-UV-MS analyses were performed at 22°C using an Agilent 1100 (Agilent Technologies, Waghaeusel-Wiesental, Germany) or a Waters Alliance 2695 (Waters SA, St-Quentin en Yvelines, France) photodiode array detector (DAD) chromatograph, respectively. A reversed-phase column (C18 Hypersil ODS, 5 μm, 100 mm × 2.1 mm; Interchim, Montluçon, France) was used at a flow rate of 0.3 mL/min. The mobile phase was composed of acetonitrile (solvent A) and acidified water (formic acid, 0.1% v/v; pH 2.6) (solvent B). Gradient: 0–5 min, 5% A; 5–30 min, 5–95% A (linear); 30–34 min, 95% A; 34–35 min, 95–5% A; 35–40 min, 5% B (equilibrium period). Under these conditions, many metabolites were separated. The injection volume was 30 μL.

The DAD-UV spectra were compared to those of certain standards (mesotrione, AMBA, MNBA) recorded at the mobile phase pH range.

LC/ESI-MS analysis

Water and acetonitrile (LC/MS grade) were obtained from J. T. Baker Laboratoires. Formic acid (LC/MS grade) was purchased from Fluka (Saint-Quentin Fallavier, France). Mesotrione as well as AMBA and MNBA analytical standards (99% purity) were a gift from Syngenta Crop Protection AG (Basel, Switzerland).

Before analysis, each sample was diluted in a mixture of water/acetonitrile (50:50) from 1/3 to 1/20 for initial concentrations of mesotrione of 1 and 5 mmol/L, respectively. Then, 30 μL were directly injected into the LC/MS system without any further treatment, using the HPLC conditions described above.

A Waters/Micromass LC/QTOF (Micromass, Manchester, UK) was used, equipped with an orthogonal geometry Z-spray ion source.

The standards as well as the supernatants were introduced into the atmospheric pressure ionization source by infusion (Harvard Apparatus, USA; flow rate 5 μL/min) or after LC separation, and ionized by ESI. Mass calibration was first performed pre-acquisition (H_3PO_4 85%; Sigma-Aldrich, Saint Quentin en Yvelines, France; 1 μL/L, 3 μL/min) and a single lock-mass correction was used during supernatant analyses (Trityrosine, Sigma-Aldrich, 5 μL/min). Possible elemental compositions were calculated for the measured masses of the intact ionized molecules and of the fragment ions and corresponding neutral losses. They were selected using the nitrogen rule and the presence of a sulfur atom and the double-bond equivalent criterion were used to check the elemental composition. Elemental compositions were selected with mass errors within 3 mDa in all but two cases which is usually acceptable for metabolite profiling in biological samples.[7] The presence of a sulfur atom was confirmed by comparison of measured and simulated isotopic ratios for M, M+1, M+2 and M+3 peaks, M corresponding to the ionized molecule. This was done using MassLynx software (Micromass, Manchester, UK). Five scans were combined before integration of the different peaks. Although isotopic ratio determinations are not accurate on a QTOF, they allowed us to confirm the presence or not of a sulfur atom.

A Waters Alliance 2695 HPLC system was used to deliver acetonitrile/acidified water solutions. The desolvation and ion source block temperatures were set at 300°C and 120°C, respectively. The source temperature as well as the sample cone position allow the formation of a stable spray and minimized the formation of droplets and water clusters. Gaseous N_2 was used as nebulizer gas (50 L/h) and desolvation gas (500 L/h). The optimum voltages found for the probe and ion source components (to produce maximum intensity) were 3 kV for the stainless-steel capillary, 35V for the sample cone, and 2V for the extractor cone. In the negative mode, voltages were switched, except the capillary voltage which was −2.1 kV for better sensitivity. Tandem mass spectrometric (MS/MS) experiments were performed by using argon in the collision cell to produce a pressure of 1 bar. A collision energy gradient (15–35 eV) was used for preliminary fingerprints and specific energies of 15–45 eV were used to unambiguously assign MS/MS

fragments. Scanning was performed from *m/z* 50–600 in the 'high resolution' mode.

Although we have written the protonated molecule as $[M+H]^+$ and the deprotonated molecule as $[M-H]^-$ for convenience, this notation is actually slightly incorrect for 'accurate mass' calculations because the addition or the loss involves a proton and not a hydrogen atom.

Synthesis of the presumed isoxazole derivative metabolite (M4)

The isoxazole derivative was prepared according to Bellamy and Ou,[11] starting from 500 mg of mesotrione and 1.7 g of $SnCl_2.2H_2O$. After the workup, a pure yellow solid precipitated during extraction with ethyl acetate. Yield: 80%.

(+)ESI-MS: *m/z* 308 ($C_{14}H_{14}NO_5S$, −0.3 mDa); (+)ESI-MS/MS *m/z* (relative ab. %): 308 (100), 291 (68), 252 (50), 229 (32), 201 (40), 190 (50). UV (H_2O, pH 2.6) λ_{max} nm: 229, 240, 249, 262, 271, 316.

^1H NMR was performed at 25°C at 500.13 MHz on an Avance 500 Bruker spectrometer (Bruker Biospin, Wissembourg, France). Water was suppressed by presaturation. Approximately 256 scans were collected (90° pulse, 7.3 μs; saturation pulse, 3 s; relaxation delay, 3 s; acquisition time, 4.679 s; 65,536 data points). Tetradeuterated sodium trimethylsilylpropionate ($TSPd_4$, Eurisotop, Saint-Aubin, France) constituted a reference for chemical shifts (0 ppm).

^1H NMR (500 MHz, H_2O/D_2O 90/10, pH = 8.0) δ ppm: 2.13 (2H, qt, CH_2); 2.61 (2H, t, CH_2); 3.28 (2H, t, CH_2); 3.39 (3H, CH_3); 8.02 (1H, dd, 1.5 Hz, 8.5 Hz); 8.56 (1H, d, 8.5 Hz); 8.85 (1H, d, 1.5 Hz).

RESULTS AND DISCUSSION

Validation of the LC/MS method

The only LC/MS method to quantify mesotrione in surface waters was proposed by Freitas *et al.* using a triple quadrupole and MeOH/acidified water (formic acid 0.1%).[12] To avoid possible reactions of the relatively reactive cyclohexanedione moiety of mesotrione metabolites with methanol (transketalization-like reactions), acetonitrile was used instead of methanol. Our gradient method was quite similar with a flow rate of 0.3 mL/min. No loss of sensitivity was observed using acetonitrile instead of MeOH. Despite the loss of sensitivity usually encountered with organic acid addition, it allowed us to observe ionization in both negative and positive modes. The sensitivity obtained in negative mode was higher for negatively charged compounds despite the presence of formic acid. Nevertheless, for a full-scan spectrum, the sensitivity in positive mode was enhanced by a factor of 2 compared to the negative mode. This compromise was guided by the need to detect both mesotrione and many unknown compounds whose 'chromatographic' and ionization properties were not known (*vide supra*). In both modes, we were able to detect several metabolites in the range 0.1–1000 μmol/L in crude mixtures (before dilution by factor 3 or 20 depending on the initial mesotrione concentration). The stable spray obtained under these conditions yielded reproducible intensities for a specific compound (data not shown).

Identification of unknown compounds by LC/MS and LC/MS/MS

MS of available reference substances

To study the behaviour of mesotrione and its two known presumed metabolites AMBA and MNBA upon fragmentation, infusions as well as LC/MS and LC/MS/MS experiments were carried out.

Mesotrione. Because of their high acidity (pK_a 3.1), the enol groups of mesotrione (Fig. 1) are completely dissociated in aqueous solution in the pH range of biodegradation (7.0–9.4). However, in LC/MS experiments, the pH of the mobile phase was 2.6. At this pH, both triketone and enolate forms may be present. Hence both positive and negative modes were used to obtained characteristic fragmentations. As mentioned above, positive ionization was possible since 0.1% of formic acid was used during the chromatographic separation. Keto-enol tautomerism is often considered as a hampering mechanism for the analysis of diketo or triketo compounds by HPLC. Chlortetracycline is a typical example of keto-enol tautomerism in which the two isomers can be separated from about 3 min with reversed-phase columns.[13] Acetylacetone was also reported to present the same phenomenon. As far as mesotrione is concerned, only one isomer was observed with an UV or MS detector, whatever the solvent used.

Protonation and deprotonation of mesotrione could theoretically occur at several positions on the keto and/or enol forms of the molecule. For example, it is possible that the $[M-H]^-$ ions observed in the (−)ESI-MS analysis could exist as either a ketone, enol, enolate or a mixture of the different forms. It may also be possible to envisage a dienol form. The complexity of such a mixture may explain the behaviour of the herbicide observed during MS/MS experiments in the (−)ESI and (+)ESI modes.

In positive mode, mesotrione (retention time (t_R) = 16.9 min) gave ions at *m/z* 340, 362 and 228 corresponding to $[M+H]^+$, $[M+Na]^+$ and $[M+H-C_6H_6O_2]^+$, respectively (Fig. 2(a)). MS^2 fragmentation of mesotrione yielded the acylium ion at *m/z* 228.

The spectrum obtained in negative mode was dominated by the ion at *m/z* 291 corresponding to loss of the nitro group. $[M-H]^-$, $[M-2H+Na]^-$ and $[2M-2H+Na]^-$ ions, at *m/z* 338, 360 and 699, respectively, were also observed. The importance of the sodium and potassium adducts observed in both modes is characteristic of di- and triketone/alkali complexes.[14]

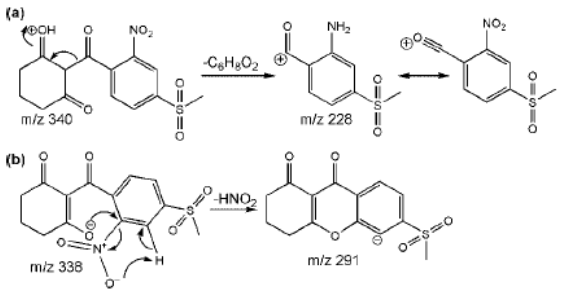

Figure 2. Proposed fragmentation pathways for mesotrione in (a) (+)ESI and (b) (−)ESI.

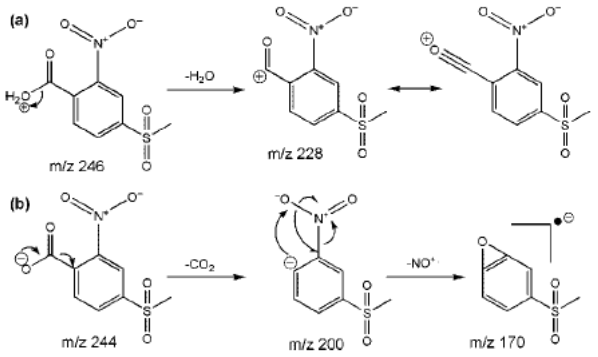

Figure 3. Proposed structures for MNBA in (a) (+)ESI and (b) (−)ESI.

Indeed, loss of a proton from a diketone/triketone results in the formation of a highly reactive diketonate that may act as an excellent chelating agent. The *m/z* 291 fragment is also observed with sulcotrione, the analogous triketone herbicide with a chlorine instead of a nitro function. Its formation might be explained by a SN_2-like reaction, as shown in Fig. 2(b). A structure for this fragment was recently reported for matrix-assisted laser desorption/ionization (MALDI): it corresponds to the formation of a triple bond in the aromatic cycle.[15] In our opinion, in the (−)ESI experiment it is easier to deprotonate the acidic proton rather than an aromatic hydrogen. However, both fragments can be envisaged.

4-Methylsulfonyl-2-nitrobenzoic acid (MNBA). The spectrum of MNBA ($t_R = 2.3$ min) revealed the presence of the dominant $[M+H-H_2O]^+$ ion in positive mode. The $[M+H]^+$ ion at *m/z* 246 was present at lower intensity than that of the sodium and dimer adducts. In negative mode, the spectrum showed ions at *m/z* 200 and 170 corresponding to the fragments $[M-H-CO_2]^-$ and $[M-H-CO_2-NO]^-$, respectively. The loss of NO corresponds to a route frequently proposed in the literature (Fig. 3).[16]

2-Amino-4-methylsulfonylbenzoic acid (AMBA). The spectrum of AMBA ($t_R = 10.1$ min) in positive mode exhibited the $[M+H-H_2O]^+$ ion at *m/z* 198 and to a minor extent the $[M+H]^+$ compound at *m/z* 216. The major fragment observed in negative mode corresponded to $[M-H-CO_2]^-$ at *m/z* 170, with the latter being the only fragment observed in the MS^2 spectrum whatever the collision energy used (15–45 eV) (Fig. 4).

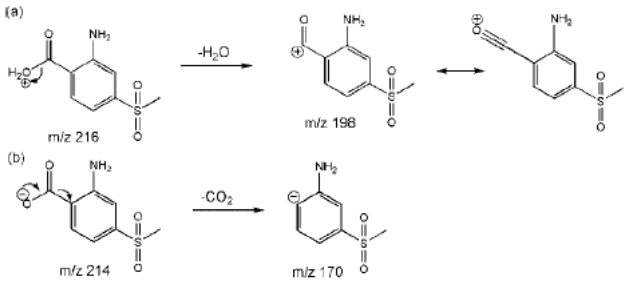

Figure 4. Proposed structures for AMBA in (a) (+)ESI and (b) (−)ESI.

Thus it could be thought that the loss of CO_2 during fragmentation in negative mode might be used as a specific marker for selective monitoring for the presence of a carboxylate group in degradation products. However, we will see that the high reactivity of triketones does not allow this conclusion with all the compounds. The methyl sulfone group does not appear to give any fragmentation, whatever the collision energy used in MS/MS experiments. This apparent stability under MS/MS conditions is in agreement with previously published results on methyl sulfone compounds from MS experiments.[17] The comparison of simulated and measured isotopic profiles and more precisely the M+2 peak was also a good indicator of the presence of the sulfur atom.

Therefore, the metabolites in the biodegradation mixtures were identified by comparison of their retention times and their characteristic MS and MS/MS data with those of standards when available (mesotrione, MNBA, AMBA).

Kinetics of mesotrione biodegradation: interpretation of the MS and MS/MS spectra

We monitored the LC/ESI-MS and LC/ESI-MS/MS behaviour of mesotrione and its degradation products at different times during incubation with the bacterial strain *Bacillus* sp. 3B6. These analyses were performed under relatively 'accurate measurement conditions' on the supernatants without any treatment to avoid loss and/or abiotic degradation of metabolites.

Whatever the initial mesotrione concentration tested in LC/MS experiments (1–5 mM), the analytical profile observed for the metabolites was nearly identical. Only the concentrations and the time courses of disappearance and appearance of metabolites changed due to lower degradation rates at higher concentrations of mesotrione.[2] In addition, the responses of both UV and MS detectors appeared to be quite similar relatively. A typical example of UV kinetics is shown in Fig. 5.

Using LC/(+)ESI-MS and LC/(−)ESI-MS, five mesotrione degradation products were observed (Figs. 5 and 6). No metabolite was observed in control experiments, whatever the ionization mode used.

Metabolite 1 (M1) was detected after only 1 h of incubation and its relative intensity increased regularly to reach a plateau at 26 h for an initial mesotrione concentration of 1 mM.

Two peaks with retention times of 11.5 (metabolite 2, M2) and 14.5 min (metabolite 3, M3) were observed after 30 min of incubation. Their concentration reached a maximum at 8 h. They decreased and progressively disappeared after 98 h and 22 h of incubation, respectively.

Another peak was observed at a retention time of 12.7 min (metabolite 4, M4). Its concentration increased to reach a maximum around 8 h then progressively decreased until the end of incubation.

A peak appeared on the total ion current (TIC) and UV chromatograms after approximately 20 h of incubation at a retention time of 12.3 min (metabolite 5, M5). This compound appeared in the incubation medium while M2 and M3, respectively, simply decreased and disappeared, plausibly suggesting transformation of the latter compound.

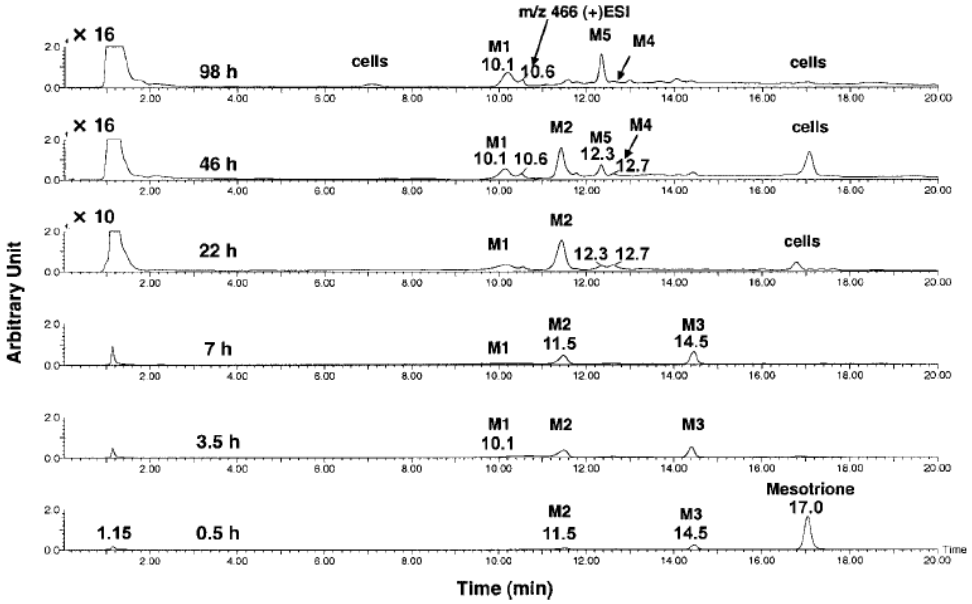

Figure 5. Degradation of 1 mM mesotrione by resting cells of *Bacillus* sp. 3B6 monitored by HPLC-UV (254 nm).

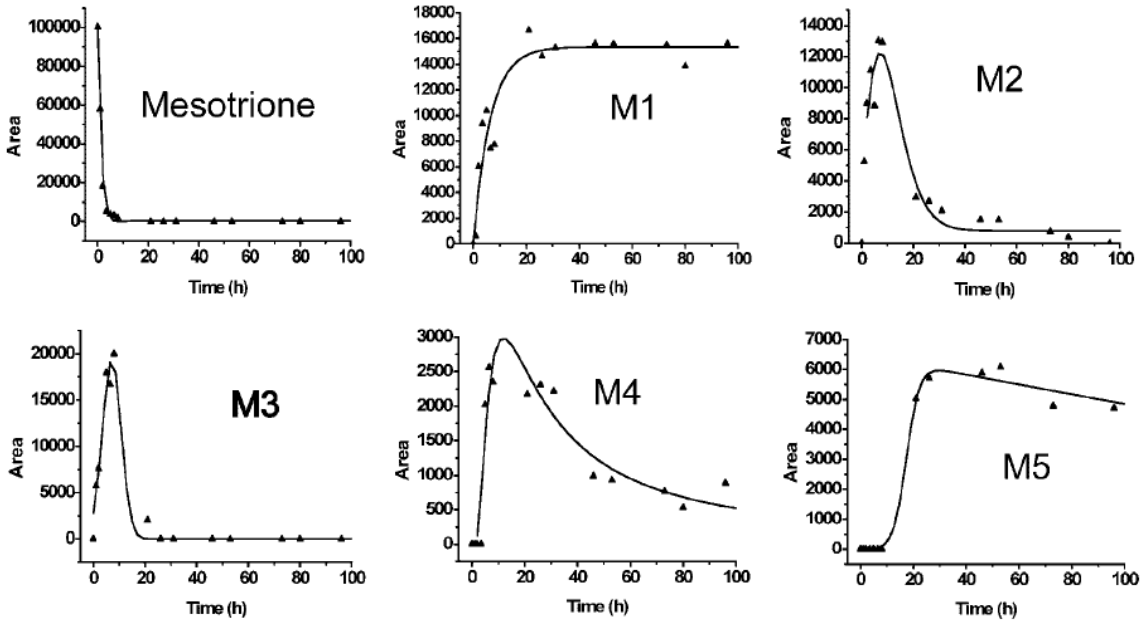

Figure 6. Time courses for mesotrione and its metabolites based on UV area (254 nm).

Finally, a peak at 10.6 min appeared after 6 h of incubation. Its level remained stable until the end of incubation.

Metabolite 1

Metabolite 1 was easily identified as AMBA on the basis of its retention time, UV spectrum and its typical fragmentations (m/z 170, $C_7H_8NO_2S^-$, −1.6 mDa; m/z 198, $C_8H_{10}NO_3S^+$, 3.0 mDa) (Tables 1 and 2).

Metabolites 2 and 3

The peaks of metabolites 2 and 3 corresponded to an ion of m/z 326 as shown by the corresponding MS spectrum in positive mode (Figs. 7(a) and 8(a)). This was confirmed by the presence of sodium and potassium adducts as well as the corresponding m/z 324 quasi-molecular $[M-H]^-$ ion observed in negative mode (Figs. 7(b) and 8(b)). These two peaks (11.5 and 14.5 min) did not correspond to the keto/enol

Table 1. Measured and calculated masses for metabolites and their fragments in (+)ESI

Metabolite	t_R (min)	Measured mass	Calculated mass	Mass error (mDa)	Elemental composition
1	10.1	198.0255	198.0225	3.0	$C_8H_{10}NO_3S^+$
2	11.5	364.0284	354.0257	2.7	$C_{14}H_{15}NO_6SK^+$
		348.0509	348.0518	−0.9	$C_{14}H_{15}NO_6SNa^+$
		326.0720	326.0698	2.2	$C_{14}H_{16}NO_6S^+$
		308.0592	308.0593	−0.1	$C_{14}H_{14}NO_5S^+$
		280.0668	280.0644	2.4	$C_{13}H_{14}NO_4S^+$
		238.0229	238.0226	0.3	$C_{11}H_{13}NO_3S^+$
3	14.5	326.0723	326.0698	2.5	$C_{14}H_{16}NO_6S^+$
		308.0606	308.0598	1.3	$C_{14}H_{14}NO_5S^+$
		238.0229	238.0233	−0.4	$C_{11}H_{13}NO_3S^+$
		212.0400	212.0381	1.9	$C_9H_{10}NO_3S^+$
4	12.7	308.0600	308.0593	0.7	$C_{14}H_{14}NO_5S^+$
5	12.3	382.0622	382.0573	4.9	$C_{14}H_{17}NO_8SNa^+$
		360.0804	360.0753	5.1	$C_{14}H_{18}NO_8S^+$
		342.0679	342.0647	3.2	$C_{14}H_{16}NO_7S^+$
		324.0571	324.0542	2.9	$C_{14}H_{14}NO_6S^+$

Table 2. Measured and calculated masses for metabolites and their fragments in (−)ESI

Metabolite	t_R (min)	Measured mass	Calculated mass	Mass error (mDa)	Elemental composition
1	10.1	214.0167	214.0174	−0.7	$C_8H_8NO_4S^-$
		170.0260	170.0276	−1.6	$C_7H_8NO_2S^-$
2	11.5	324.0549	324.0542	0.7	$C_{14}H_{14}NO_6S^-$
		280.0618	280.0644	−2.6	$C_{13}H_{14}NO_4S^-$
		201.0820	201.0790	3.0	$C_{12}H_{11}NO_2^{\cdot -}$
3	14.5	346.0387	346.0361	2.6	$C_{14}H_{13}NO_6SNa^-$
		324.0557	324.0542	1.5	$C_{14}H_{14}NO_6S^-$
		210.0231	210.0225	0.6	$C_9H_8NO_3S^-$
4	12.7	306.0600	306.0593	0.7	$C_{14}H_{12}NO_5S^-$
5	12.3	380.0405	380.0416	−1.1	$C_{14}H_{15}NO_8SNa^-$
		358.0604	358.0597	0.7	$C_{14}H_{16}NO_8S^-$
		214.0210	214.0174	3.6	$C_8H_8NO_4S^-$
		170.0286	170.0276	1.0	$C_7H_8NO_2S^-$

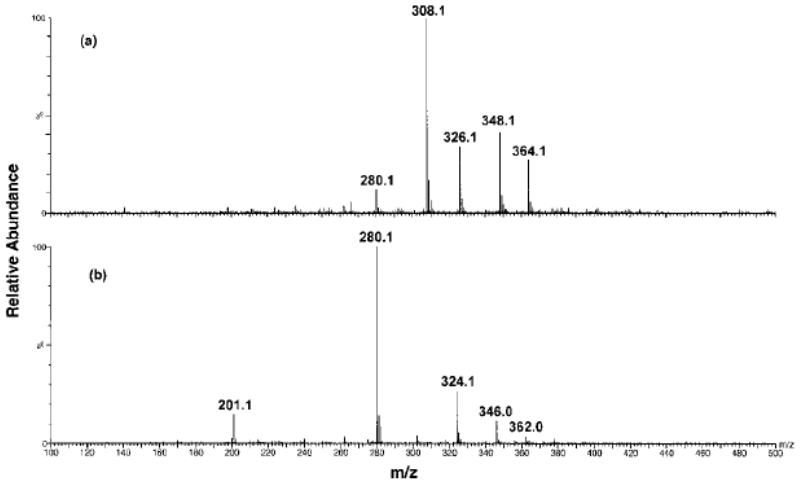

Figure 7. MS spectra of M2 recorded after 22 h of incubation in (a) (+)ESI and (b) (−)ESI.

form since the peak with a $t_R = 14.5$ min disappeared after 22 h of incubation while that with a $t_R = 11.5$ min was still present. The elemental compositions found for the compounds appearing at 11.5 and 14.5 min were $C_{14}H_{16}NO_6S^+$ with a mass error of 2.2 and 2.5 mDa, respectively (Table 1). The isotopic ratio confirmed the presence of a sulfur atom (data not shown).

A typical biotransformation pathway of nitro aromatic compounds by microorganisms is the reduction of the nitro moiety to the corresponding nitroso, hydroxylamine and/or

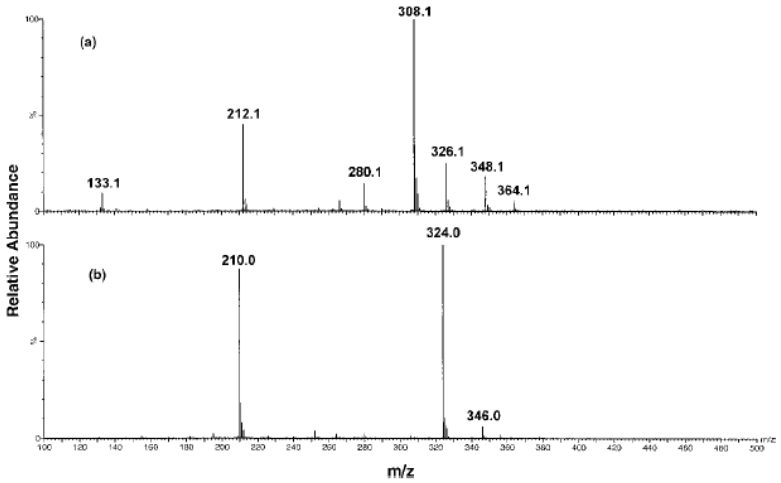

Figure 8. MS spectra of M3 obtained after 7 h of incubation in (a) (+)ESI and (b) (−)ESI.

amine function.[18] In the present case, the mass measured indicates the presence of hydroxylamine-like compounds. This kind of reaction can occur under anaerobic and aerobic conditions since nitroreductases are ubiquitous enzymes.[18–22]

The M2 ion presented several in-source fragmentations: *m/z* 308 ($C_{14}H_{14}NO_5S^+$, −0.1 mDa) and 280 ($C_{13}H_{14}NO_4S^+$, 2.4 mDa) in positive mode and *m/z* 280 ($C_{13}H_{14}NO_4S^-$, −2.6 mDa) in negative mode (Tables 1 and 2). The presence of a sulfur atom was confirmed for all fragments by isotopic ratio determination.

To confirm this hypothesis, MS/MS studies were undertaken both in positive and negative mode. Fragmentation of *m/z* 326 led to formation of *m/z* 308, 280 and 238 fragments. The *m/z* 308 MS/MS experiment led to formation of the *m/z* 280 and 238 ions while collision of the *m/z* 280 led to formation of the *m/z* 238 ion. In negative mode, fragmentation of the *m/z* 324 ion led to formation of fragments at *m/z* 280 and 201 ($C_{12}H_{11}NO_2^{-\cdot}$, 3.0 mDa) (Table 2), the latter being a fragmentation of *m/z* 280. The odd mass observed implies the presence of an anion radical. And, analysis of the isotopic ratios confirmed the absence of a sulfur atom.

Similar experiments carried out on M3 gave the following sequences: *m/z* 326 → 308 ($C_{14}H_{14}NO_5S^+$, 1.3 mDa) → 280 → 238 ($C_{11}H_{13}NO_3S^+$, −0.4 mDa) and *m/z* 308 → 212 ($C_9H_{10}NO_3S^+$, 1.9 mDa) in positive mode (Fig. 7(a)) and *m/z* 324 ($C_{14}H_{14}NO_6S^-$, 1.5 mDa) → 280 as well as *m/z* 324 → 210 ($C_9H_8NO_3S-$, 0.6 mDa) in negative mode (Fig. 7(b)). Fragments at *m/z* 212 and 133 obtained in (+)ESI were produced both in-source and during MS/MS experiments. It should be noted that a sample cone voltage of 15 V (instead of 35 V) changed the relative abundances with a dominant ion at *m/z* 326.

If we consider the possibility of tautomerism for the hydroxylamine function, in conjunction with the presence of a keto group in the gamma position, the scheme shown in Fig. 9 must be considered.

This type of equilibrium has been described in the literature and studied by time-resolved infrared (IR) and UV spectroscopies on different molecules.[23–25] The ring-chain tautomerism (cyclized or open) is modulated by substituent effects. In the presence of a keto function, the open form is stabilized by a strong intramolecular (internal) hydrogen bond.[23] This equilibrium can be described well by UV spectra. Cyclized forms are characterized by an absorption band at 315 nm while the linear form presents a band around 355–365 nm.[23]

In our study, the UV spectra of M2 and M3 presented absorption bands at 355 and 316 nm corresponding to the linear and ring forms, respectively. In addition, we observed that M3 was degraded under abiotic conditions (after cell harvesting) within approximately 12 h (data not shown) since its area decreased when the sample was kept at room temperature for that length of time. This is in agreement with the presence of the relatively unstable isoxazol-3-ol compound, certainly easily converted into its isoxazole form by dehydration under aerobic conditions. These results agree with the different conjectured fragmentation pathways for hydroxylamine and isoxazol-3-ol ions as shown in Figs. 10 and 11, respectively.

The loss of 18 Da observed in (+)ESI (Figs. 10(a) and 11(a)) can be explained by dehydration which can easily occur with hydroxylamine and isoxazol-3-ol. The consecutive loss of CO

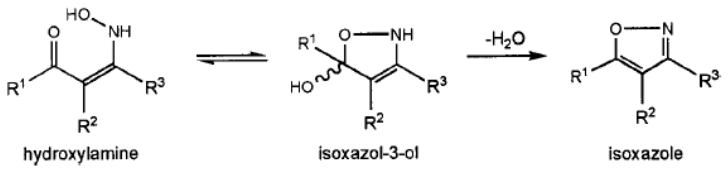

Figure 9. Tautomerism encountered with γ-ketohydroxylamine derivatives.

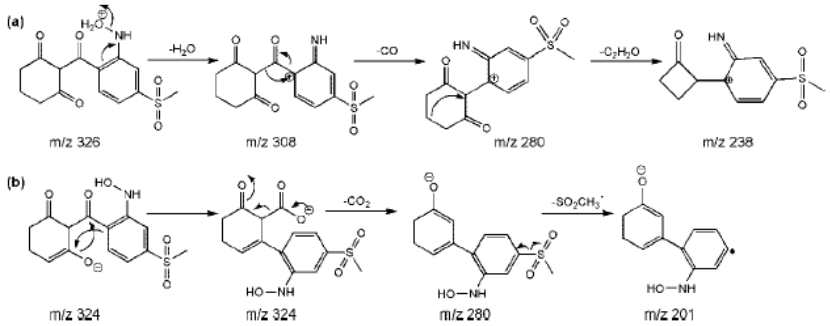

Figure 10. Proposed fragmentation pathways for hydroxylamine (M2) in (a) (+)ESI and (b) (−)ESI.

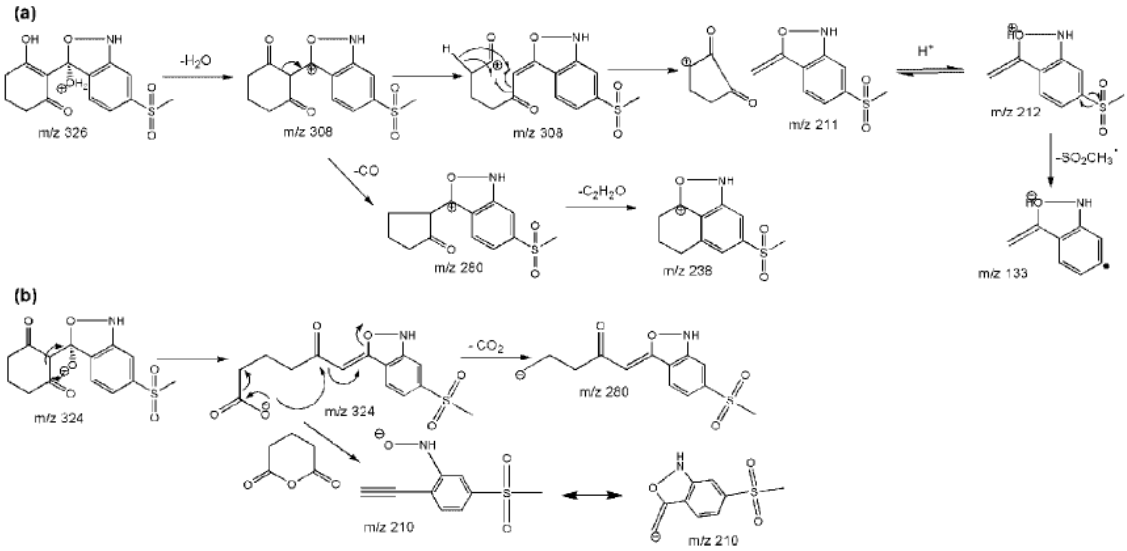

Figure 11. Proposed fragmentation pathways for isoxazol-3-ol (M3) in (a) (+)ESI and (b) (−)ESI.

and C_2H_2O is a quite common mechanism suggested for 'cycloalkanone'-like compounds, generating successive ring cleavages.[26,27]

In LC/(−)ESI-MS/MS experiments, the main fragment observed for the hydroxylamine (M2) corresponded to the neutral loss of CO_2, yielding an ion of *m/z* 280. Fragmentation of this type is often encountered in β-diketone (−)ESI-MS/MS fragmentations. As an example, such a mechanism was recently reported on some curcuminoids.[28] Taking into account the strength of the N–O bond of the hydroxylamine functions and their relatively high basicity, it is more reasonable to envisage a rearrangement from one of the possible enolate forms to yield a conjugated product ion at *m/z* 280. The loss of the methyl sulfone moiety from the precursor ions of *m/z* 280 by homolytic cleavage led to the formation of an anion radical of *m/z* 201 as shown by the MS/MS experiment. This fragmentation involving a radical was not observed for the other methyl sulfone derivatives previously. It may be explained by the relative high stability of this radical due to strong conjugation.

As far as isoxazol-3-ol is concerned, one of the mechanisms proposed for (+)ESI fragmentation involved dehydration of the tertiary alcohol (leading to *m/z* 308), followed by rearrangement, resulting in a fragment at *m/z* 212 (Fig. 11(a)). This ion was observed during in-source fragmentation and during MS/MS experiments. The *m/z* 212 ion appeared to be quite stable in our mechanism, justifying its presence in-source. Another minor fragment was observed at *m/z* 133 both in-source and during MS/MS experiments. It corresponded to loss of the methyl sulfone group with a radical mechanism from the *m/z* 212 fragment. An ion of *m/z* 280 was also observed. Its formation involved a second fragmentation pathway with the loss of CO from the *m/z* 308 fragment. However, further experiments performed on another source and/or analyzer might be useful to clarify the full fragmentation pathway of the *m/z* 308 ion. It should be noted that it was not possible under our conditions to detect unambiguously whether one sequential (*m/z* 308 → 280 → 212) or two parallel (*m/z* 308 → 212) pathways existed for generation of the *m/z* 212 ion.

In (−)ESI-MS/MS experiments, the formation of product ions of *m/z* 280 and 210 can be explained by two competitive pathways: one involving the loss of CO_2 (leading to *m/z* 280) and the other an internal rearrangement of isoxazol-3-ol (Fig. 11(b)). The *m/z* 210 ion corresponds to the most stable product. This is a reasonable supposition when we consider

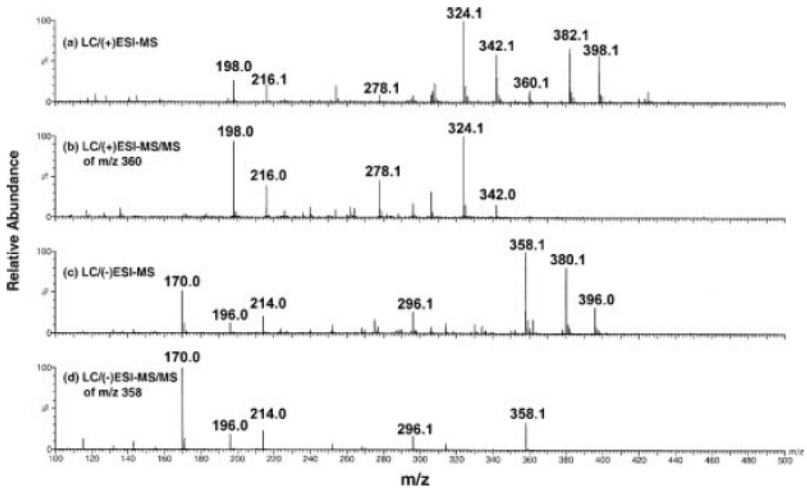

Figure 12. MS spectra of M5 (98 h of incubation).

its highly conjugated structure. Due to its apparent instability under aerobic conditions (data not shown), isoxazol-3-ol may be converted into isoxazole after dehydration, yielding a *m/z* 308 ion in positive mode.

Metabolite 4

A ion of *m/z* 308 was successfully observed in all kinetics at 12.7 min (M4) and confirmed by the presence of a *m/z* 306 fragment in negative mode. The elemental composition found for this metabolite was $C_{14}H_{14}NO_5S^+$ with a mass error of 0.7 mDa (Table 1). To confirm this hypothesis, isoxazole was synthesized by a Clemensen-like reduction and co-eluted with the samples.[11] The synthetic compound presents the same retention time, UV and mass spectrum as that observed in the supernatants. It should be noted that the UV spectrum of this compound presents an absorption band at 316 nm, i.e. at the same λ_{max} as isoxazol-3-ol. This constitutes more evidence of the cyclized structure of isoxazol-3-ol.

Moreover, MS/MS experiments confirmed the similarity between the two compounds since both presented fragments of low intensity: *m/z* 308 (100%), 291 (68%), 252 (50%), 229 (32%), 201 (40%), and 190 (50%). It should be noted that this ion (*m/z* 308) is not easily fragmented. It does not correspond to those formed during in-source fragmentation of hydroxylamine or isoxazol-3-ol (M2 and M3) which do not present the same MS^2 patterns. The latter are easily fragmented in-source.

Finally, the presence of such a compound (proven by comparison with a synthetic standard) is indirect evidence of the presence of hydroxylamine. The isoxazole may be the result of the abiotic evolution of the ring-chain tautomerism equilibrium. Intramolecular cyclization was recently observed during phototransformation of sulcotrione (chlorine homologue of mesotrione), in which enol and chlorine functions play the roles of 'nucleophile' and 'electrophile', respectively.[29] However, photochemical mechanisms obviously cannot be compared with those obtained under biotic conditions.

Metabolite 5

The LC/ESI-MS and LC/ESI-MS/MS spectra of metabolite 5 (M5) are presented in Fig. 12. Comparison of positive and negative modes allowed us to identify *m/z* 360 ($C_{14}H_{18}NO_8S^+$, 5.1 mDa) and 358 ($C_{14}H_{16}NO_8S^-$, 0.7 mDa) as the $[M+H]^+$ and the $[M-H]^-$ quasi-molecular ions, respectively (Tables 1 and 2).

The presence of sodium and potassium adducts may indicate a diketone/alkali complex as mentioned above.[14] In addition, the loss of water molecules in-source in positive mode, leading to fragments at *m/z* 342 ($C_{14}H_{16}NO_7S^+$, 3.2 mDa) and 324 ($C_{14}H_{14}NO_6S^+$, 2.9 mDa), allows us to consider the presence of carboxylic acid, secondary alcohol and/or hydroxylamine functions. Fragments at *m/z* 216 and 198, identical to those of AMBA, were also observed. The major fragments observed in LC/(+)ESI-MS/MS experiments were *m/z* 324 and 198. Minor fragments at *m/z* 278 and 216 were also observed. In LC/(−)ESI-MS/MS, the dominant fragment was an ion at *m/z* 170 ($C_7H_8NO_2S^-$, 1.0 mDa), a minor fragment at *m/z* 214 ($C_8H_8NO_4S^-$, 3.6 mDa) being also detected (Table 2). Once again, these fragments corresponded to those observed for AMBA in negative mode, indicating a similar structure.

Sulcotrione (belonging to the same family of herbicides as mesotrione but with a chlorine atom instead of a nitro function) has been reported to be biotransformed after an oxidative cleavage of the cyclohexanedione moiety resulting in the formation of a carboxylic acid.[30] Moreover, this type of cleavage corresponds to a general biodegradative pathway of 1,2-diketone or 1,3-triketone.[31–33] Similar mechanisms are usually encountered during cyclohexanol metabolism.[31] The first step can be a oxidation, yielding cyclohexanone. This ketone is then hydroxylated in the β position from the keto group, yielding a secondary alcohol which is in its turn oxidized before cleavage of the C_1–C_2 bond.

Based on this hypothesis, 'oxidative mechanisms' such as these have been considered, leading to the possible metabolite 5 (Fig. 14), in agreement with the elemental

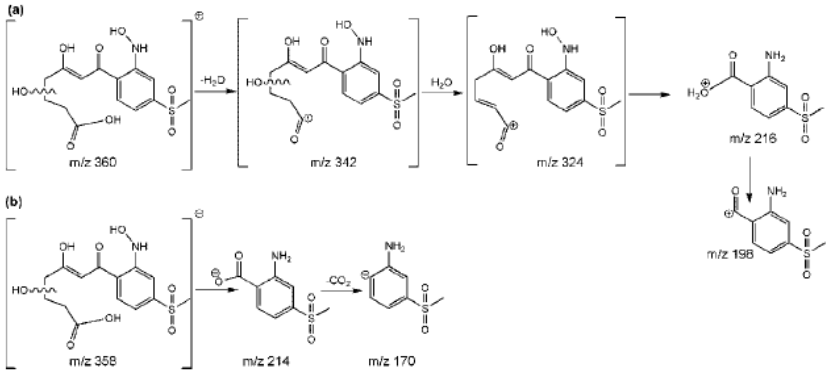

Figure 13. Possible fragmentation pathways for M5 in (a) (+)ESI and (b) (−)ESI.

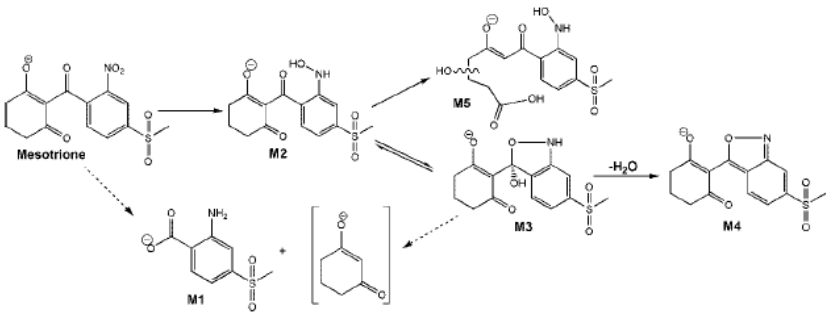

Figure 14. Proposed mesotrione metabolic pathway by *Bacillus* sp. 3B6.

formula $C_{14}H_{16}NO_8S^-$ obtained within 0.7 mDa in negative mode. The fragments formed in-source or during MS/MS confirmed this hypothesis. Fragmentation pathways are proposed in Fig. 13.

Reduction of nitro to amine (predicted at *m/z* 310 in (+)ESI-MS) was also considered as a potential pathway, since many reduced compounds have been described in the literature. However, similar compounds bearing an amino group were not detected in our study regardless of the ionization conditions used. Moreover, it is well known that arylhydroxylamines are relatively difficult to reduce to amines because the N–O bond is strengthened by electron-withdrawing groups. Therefore, the rate of reduction to amine is slower than that of formation of hydroxylamine. This type of reactivity has recently been reported in the literature during biotransformation of aromatic nitro compounds by baker's yeast or plant cells.[34,35]

Another metabolite detected

Finally, a peak at 10.6 min with an apparent mass of 465 appeared after 6 h of incubation. This relatively high molecular weight compound may be explained by the formation of a glutathione or a glucuro conjugate. However, neither a glutathione nor glucuronic acid derivative would result in such an ion being observed. Moreover, glucuro conjugates are not usually described in prokaryote cell metabolism. Thus, the dimerization of a precursor metabolite has been considered. Indeed, dimerization of hydroxylamino compounds can occur under biotic or abiotic conditions leading to an azo bond.[21,36] The UV spectrum of the 10.6 min compound presents two absorption bands at 420 and 530 nm, in agreement with the formation of a highly conjugated azo compound. Further investigations will be necessary to determine the structure of this metabolite more completely. For example, *in situ* NMR measurements performed directly on the incubation medium may be useful to clarify the structure. Otherwise, preparative HPLC will be necessary. Finally, a new metabolic pathway can be proposed (Fig. 14). This proposed scheme is consistent with the time courses of mesotrione and its metabolites (Fig. 6).

MNBA was never observed under our LC/MS conditions although it has been detected in soil samples and proposed as a potential metabolite in other studies. Moreover, we observed (data not shown) that MNBA was slowly biotransformed into AMBA in resting cell experiments. Two hypotheses can be proposed: (i) MNBA is formed at concentrations below the detection limit of our method and (ii) MNBA does not accumulate in the medium, being transformed as soon as it is formed.

CONCLUSIONS

A full description of mesotrione herbicide biotransformation is given for the first time by LC/ESI-MS and LC/ESI-MS/MS experiments in both positive and negative modes. Five metabolites were identified in crude incubation media, among them four, never described before, were identified by their elemental composition, MS^2 fragments as well as isotopic patterns. They all correspond to a reduction of the nitro function, with two belonging to the hydroxylamine

compound family. It should be noted that arylhydroxylamine compounds are considered to be potentially mutagenic.[37,38] Therefore, the results presented here constitute an important step for monitoring the fate of mesotrione in the environment.

From a chemical point of view, the high reactivity of this triketone herbicide was confirmed by its high reactivity as an electrophilic centre, leading, for example, to an isoxazole derivative. This reactivity plays an important role in the biotic and abiotic transformation mechanisms as well as in the fragmentation pathways observed in ESI for each metabolite identified. Quantum chemistry calculations may provide useful information on these fragmentation pathways. Finally, MNBA was not identified under our conditions although it was suggested to be one of the major metabolites in the literature along with the ability of the *Bacillus* sp. 3B6 strain to biotransform MNBA. A comparative study using *in situ* ^{1}H NMR spectroscopy is in progress to obtain further information concerning the full metabolic pathways, especially to detect metabolites not responding to ESI, and to specify the type of nitroreductase involved.

Acknowledgements

S. Durand is the recipient of a fellowship from the French Ministère de la Recherche. The authors acknowledge Syngenta Crop Protection AG for the gift of standards.

REFERENCES

1. Mitchell G, Bartlett DW, Fraser TEM, Hawkes TR, Holt DC, Townson JK, Wichert RA. *Pest. Manag. Sci.* 2001; **57**: 120.
2. Durand S, Amato P, Sancelme M, Delort A-M, Combourieu B, Besse-Hoggan P. *Lett. Appl. Microbiol.* 2006; **43**: 222. DOI: 10.1111/j.1472-765X.2006.01923.x.
3. Rouchaud J, Neus O, Eelen H, Bulcke R. *Med. Fac. Landbouww. Univ. Gent* 2000; **65/2a**: 51.
4. Dyson JS, Beulke S, Brown CD, Lanes MCG. *J. Environ. Qual.* 2002; **31**: 613.
5. Gledhill AJ, Jones BK, Laird WJD. *Xenobiotica* 2001; **31**: 733.
6. Alferness P, Wiebe L. *J. Agric. Food Chem.* 2002; **50**: 3926.
7. Suzuki S, Ishii T, Yasuhara A, Sakai S. *Rapid Commun. Mass Spectrom.* 2005; **19**: 3500.
8. Boernsen KO, Gatzek S, Imbert G. *Anal. Chem.* 2005; **77**: 7255.
9. Pilard S, Caradec F, Jackson P, Luijten W. *Adv. Mass Spectrom.* 2001; **15**: 687.
10. Von Roepenack-Lahaye E, Degenkolb T, Zerjeski M, Franz M, Roth U, Wessjohann L, Schmidt J, Scheel D, Clemens S. *Plant Physiol.* 2004; **134**: 548.
11. Bellamy FD, Ou K. *Tetrahedron Lett.* 1984; **25**: 839.
12. Freitas LG, Götz CW, Ruff M, Singer HP, Muller SR. *J. Chromatogr. A* 2004; **1028**: 277.
13. Cherlet M, Croubels S, De Backer P. *J. Chromatogr. A* 2006; **1102**: 116.
14. Hall BJ, Brodbelt JS. *J. Am. Soc. Mass Spectrom.* 1999; **10**: 402.
15. Mullen AK, Clench MR, Crosland S, Sharples KR. *Rapid Commun. Mass Spectrom.* 2005; **19**: 2507.
16. Williams TTJ, Perreault H. *Rapid Commun. Mass Spectrom.* 2000; **14**: 1474.
17. Jemal M, Hawthorne D. *Rapid Commun. Mass Spectrom.* 1999; **13**: 61.
18. Ye J, Singh A, Ward OP. *World J. Microbiol. Biotechnol.* 2004; **20**: 117.
19. Hughes JB, Wang CY, Zhang C. *Environ. Sci. Technol.* 1999; **33**: 1065.
20. Subramanian M, Oliver DJ, Shanks JV. *Biotechnol. Prog.* 2006; **22**: 208.
21. Pak JW, Knoke KL, Noguera DR, Fox BG, Chambliss GH. *Appl. Environ. Microbiol.* 2000; **66**: 4742.
22. Somerville CC, Nishino SF, Spain JC. *J. Bacteriol.* 1995; **177**: 3837.
23. Barth A, Corrie JET, Gradwell MJ, Maeda Y, Mäntele W, Meier T, Trentham DR. *J. Am. Chem. Soc.* 1997; **119**: 4149.
24. Uncuta C, Tudose A, Caproiu M, Udrea S, Roussel C. *Eur. J. Org. Chem.* 2003; **9**: 1789.
25. Fabian WMF, Schweiger K, Weis R. *J. Phys. Org. Chem.* 1999; **12**: 635.
26. March RE, Miao X-S. *Int. J. Mass Spectrom.* 2004; **231**: 157.
27. Es-Safi N-E, Kerhoas L, Ducrot P-H. *Rapid Commun. Mass Spectrom.* 2005; **19**: 2734.
28. Jiang H, Somogyi A, Jacobsen NE, Timmermann BN, Gang DR. *Rapid Commun. Mass Spectrom.* 2006; **20**: 1001.
29. Ter Halle A, Drncova D, Richard C. *Environ. Sci. Technol.* 2006; **40**: 2989.
30. Rouchaud J, Neus O, Bulcke R, Cools K, Eelen H. *Bull. Environ. Contam. Toxicol.* 1998; **61**: 669.
31. Grogan G. *Biochem. J.* 2005; **388**: 721.
32. Hoehle SI, Pfeiffer E, Solyom AM, Metzler M. *J. Agric. Food Chem.* 2006; **54**: 756.
33. Straganz G, Brecker L, Weber H-J, Steiner W, Ribbons DW. *Biochem. Biophys. Res. Commun.* 2002; **297**: 232.
34. Li F, Cui J, Qian X, Zhang R. *Chem. Commun.* 2004; **20**: 2338.
35. Li F, Cui J, Qian X, Zhang R, Xiao Y. *Chem. Commun.* 2005; **14**: 1901.
36. March J. In *Advanced Organic Chemistry, Reactions, Mechanisms, and Structure* (4th edn). John Wiley, Wiley Interscience, 1992; 638–639.
37. Benigni R, Giuliani A, Franke R, Gruska A. *Chem. Rev.* 2000; **100**: 3697.
38. Guengerich FP. *Drug Metab. Rev.* 2002; **34**: 607.